J. Fluid Mech. (1991), *vol.* 232, *pp.* 455–467
Printed in Great Britain

Model computations of the influence of carbon impurities on the ionization relaxation in krypton shock waves

By D. KLAGES AND F. DEMMIG
Institut für Plasmaphysik, Universität Hannover, Callinstraße 38, D-3000 Hannover, Germany

(Received 13 May 1990 and in revised form 12 December 1990)

Chemical reactions in shock waves can be strongly affected by minute impurity concentrations. Thus it is not adequate to take into account the additional impurity electron production in relaxation studies simply by global adjustment of the atom–atom excitation cross-section constant to the measured electron density.

A definite improvement, however, can only be achieved if the ionization relaxation model is extended to include all relevant impurity atom reactions. Consequently we treated the real test gas as a mixture of krypton and impurity carbon atoms. For the carbon model it is important to take the lower real excitation levels into consideration. Carrying out a sensitivity analysis we were able to reduce the number of reactions substantially. A comparison with experimental electron density profiles yielded 3.0×10^{-6} m^2/J for the Kr–Kr excitation cross-section constant as well as values for the C–Kr constants.

For a temperature of about 8000 K and an impurity concentration of about 40 p.p.m. it is shown that the impurity reactions dominate the electron production in the initial relaxation zone. This effect causes a pronounced decrease of the relaxation time with increasing concentration.

By comparing computational results of the Kr–C model with those of the simplistic pure Kr model it is possible to explain the dependence of the Kr–Kr excitation cross-section constant on the impurity concentration and the plasma temperature.

1. Introduction

The influence of impurities on rare-gas shock waves has been studied by a number of authors, e.g. Glass, Liu & Tang (1977) who investigated the influence of hydrogen impurities in the per cent region on shock structure, stability and the ionization relaxation in krypton shock waves at Mach numbers $M_S \gtrsim 15$. Regarding the ionization relaxation Igra (1972) has already pointed out that impurities of the test gas can give rise to a considerable increase of the electron density within the relaxation zone due to additional electron production by impurity atoms. Chemical reactions in shock waves generally can be severely affected even by minute impurity concentrations as has been investigated, for example, by Lifshitz & Bidani (1981). In such a case it is difficult or even impossible to draw conclusions from experimental data regarding, for example, rate coefficients or cross-sections of the test gas. In the case of ionization relaxation, test gas impurities cannot be reduced to an arbitrary low level. As a consequence, the electron density of the initial relaxation zone is determined by impurity reactions if the ionization energy of the impurity atom is

markedly lower than that of the test gas atom. The excitation and ionization reactions of the test gas atoms to be investigated are then nearly totally screened.

If the influence of impurities is treated as a source of a systematical error, only a rough upper bound for the atom–atom collisional excitation and ionization cross-sections of the test gas can be derived. Thus, in the history of shock tube experiments with krypton the collisional excitation cross-section constant has decreased by a factor of 50 merely by improvement of experimental conditions by reducing the impurity concentration from a few hundred p.p.m. to the p.p.m. range. A definite improvement, however, can only be achieved if the ionization relaxation model is extended to comprise all relevant impurity atom reactions. Consequently, we treated the real test gas as a mixture of krypton and carbon atoms, the latter being the main contributor to the impurities in our case.

2. Ionization relaxation model

Since our main concern is the investigation of ionization relaxation in shock tube plasmas we confine ourselves to one-dimensional flow (Demmig 1983*b*). In order to describe the influence of impurities a gas mixture is assumed and the flow is treated as unsteady in view of shock attenuation (Demmig 1983*a*, *b*). The effect of wall boundary layers on the free flow is taken into account approximately by a mass loss term using a boundary-layer factor of 1.7. This commonly used approximation has most recently been refined by Meißner (1988) who treated the two-dimensional boundary layers rigorously for a single flow. Since we are mainly interested in the implications of impurities regarding the reaction kinetics, the boundary-layer model applied does not have crucial influence.

We applied our model to shock tube experiments in krypton at plasma temperatures (i.e. the Rankine–Hugoniot temperature T_{A0}) in the range of 7500–13000 K. Hence it is justified to neglect radiation processes within the relaxation zone as well as multiple ionization. Moreover the precursor electron density values at the shock front as determined by Krauß-Varban (1985) with an unsteady precursor model have a negligible effect on the relaxation time. For our maximum Mach number it is less than 0.2%. In view of the experimental conditions we study impurity concentrations in the low p.p.m. range. A summary of typical data for three different shock tube experiments is listed in table 1.

We choose a two-step model for the test gas atom Kr as well as for the impurity atom C in order to describe the ionization relaxation by a compact model. The energy of the model excitation level of krypton comprising the 5 s-states amounts to 10.18 eV (Krauß-Varban & Demmig 1984). For the ionization energy of krypton atoms we use a value of 14.0 eV. For the carbon model illustrated in figure 1, it is vital to take the lower real excitation levels into consideration. The statistical weights of the model levels are g^0, g^*, and g^+, respectively. The energy of the ground-state model level comprising the lowest real excitation level $2p^2\ {}^1\mathrm{D}$ is 0.45 eV. Consequently in our model the ionization energy of a C atom amounts to 10.81 eV (figure 1).

In the outset of our investigations we took 21 collision reactions into consideration. Therefore we used a special notation for reaction rates, cross-section constants, etc. Carbon particles, krypton particles and electrons are denoted by C, K, and e, respectively. The ground state, the excited state and the ground state of the singly ionized heavy particles are denoted by the superscripts 0, * and +, respectively. As an example, the excitation rate of carbon atoms in the ground state colliding with ground-state krypton atoms is denoted by $R^{*}_{C^0K^0}$. Here, the subscripts indicate the

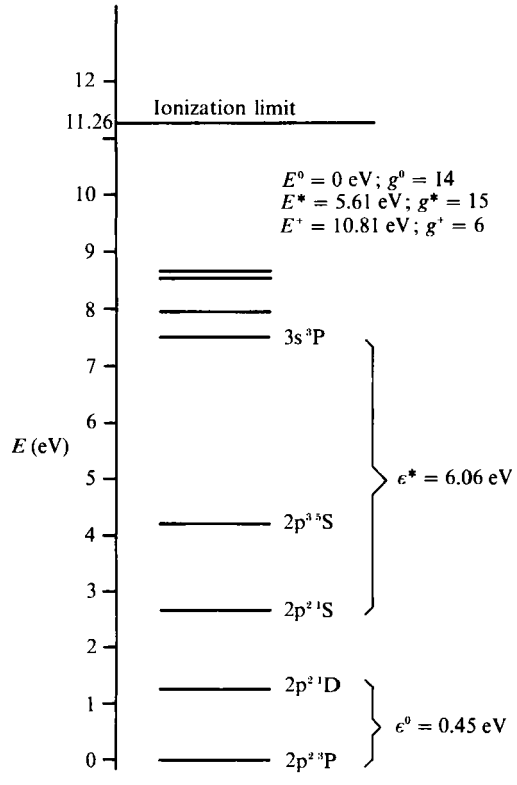

FIGURE 1. Model levels of C.

P_0 (hPa)	M_S	T_{A0} (K)	T_{e0} (K)	η (p.p.m.)
53.5	8.89	7567.2	7430.9	37.5
13.2	10.08	9626.4	8695.8	37.5
10.6	11.77	13008.5	9762.5	16.2

TABLE 1. Values of the initial pressure, P_0, Mach number, M_S, heavy particle temperature, T_{A0}, electron temperature, T_{e0}, and impurity concentration, η, for typical experimental conditions. The values of M_S, T_{A0}, and T_{e0} refer to a fixed measurement station.

colliding particles in their respective initial states. Since the second particle is assumed not to change the electronic state during a collision, the superscript indicates the final state of the first particle. The rate equations for the excitation/ionization processes then read

$$\dot{n}_{K^*} = R^*_{K^0K^0} - R^+_{K^*K^0} + R^*_{K^0e} - R^+_{K^*e}, \tag{2.1}$$

$$\dot{n}_{C^+} = R^+_{C^*K^0} + R^+_{C^*e}, \tag{2.2}$$

$$\dot{n}_{C^0} = -R^*_{C^0K^0} - R^*_{C^0e}, \tag{2.3}$$

$$\dot{n}_{C^*} = R^*_{C^0K^0} - R^+_{C^*K^0} + R^*_{C^0e} - R^+_{C^*e}, \tag{2.4}$$

$$\dot{n}_e = R^+_{K^0K^0} + R^+_{K^*K^0} + R^+_{C^*K^0} + R^+_{K^*e} + R^+_{C^*e}. \tag{2.5}$$

The partial rates of the reactions are given by

$$R^{*}_{K^0K^0} = (n_{K^0})^2 S^{*}_{K^0K^0} - n_{K^*} n_{K^0} S^{0}_{K^*K^0}, \tag{2.6}$$

$$R^{+}_{K^*K^0} = n_{K^*} n_{K^0} S^{+}_{K^*K^0} - n_{K^+} n_{K^0} n_e S^{*}_{K^+K^0}, \tag{2.7}$$

$$R^{+}_{K^0K^0} = (n_{K^0})^2 S^{+}_{K^0K^0} - n_{K^+} n_{K^0} n_e S^{0}_{K^+K^0}, \tag{2.8}$$

$$R^{*}_{C^0K^0} = n_{C^0} n_{K^0} S^{*}_{C^0K^0} - n_{C^*} n_{K^0} S^{0}_{C^*K^0}, \tag{2.9}$$

$$R^{+}_{C^*K^0} = n_{C^*} n_{K^0} S^{+}_{C^*K^0} - n_{C^+} n_{K^0} n_e S^{*}_{C^+K^0}, \tag{2.10}$$

$$R^{*}_{K^0e} = n_e n_{K^0} S^{*}_{K^0e} - n_{K^*} n_e S^{0}_{K^*e}, \tag{2.11}$$

$$R^{+}_{K^*e} = n_{K^*} n_e S^{+}_{K^*e} - n_{K^+} (n_e)^2 S^{*}_{K^+e}, \tag{2.12}$$

$$R^{*}_{C^0e} = n_{C^0} n_e S^{*}_{C^0e} - n_{C^*} n_e S^{0}_{C^*e}, \tag{2.13}$$

$$R^{+}_{C^*e} = n_{C^*} n_e S^{+}_{C^*e} - n_{C^+} (n_e)^2 S^{*}_{C^+e}, \tag{2.14}$$

where n_{K^0}, n_{K^*}, n_{K^+}, n_{C^0}, n_{C^*} and n_{C^+} are the corresponding heavy particle densities and n_e the electron density, respectively. S denotes the rate coefficient of a specific reaction. The rate coefficient is given by

$$S^{k}_{ij} = \int\int f_i(V_i) f_j(V_j)\, G Q^{k}_{ij}(G)\, \mathrm{d}^3 V_i\, \mathrm{d}^3 V_j, \tag{2.15}$$

with

$$G = |V_i - V_j|, \tag{2.16}$$

where $f_i(V_i)$ and $f_j(V_j)$ are the velocity distributions of the collision partners i and j, G is the magnitude of the relative velocity of i and j, and $Q^{k}_{ij}(G)$ is the corresponding collision cross-section. The superscript k indicates the final state of particle i. Under the assumption of a linear increase of the collision cross-section above the threshold energy E_{th} with the relative kinetic energy of the collision partners E

$$Q^{k}_{ij}(E) = C^{k}_{ij}(E - E_{th}) \tag{2.17}$$

and a Maxwell distribution of both electrons and heavy particles, equation (2.15) yields

$$S^{k}_{ij} = 4C^{k}_{ij}(2\pi\mu)^{-\frac{1}{2}}(KT_n)^{\frac{1}{2}}(E_{th} + 2KT_n)\exp(-E_{th}/KT_n) \tag{2.18}$$

(Krauß-Varban 1985), where C^{k}_{ij} is the cross-section constant of the collision process, K is the Boltzmann constant, and μ and T_n are the reduced mass of the collision particles and the electron temperature or the heavy particle temperature, respectively.

The assumption of a linearly increasing cross-section (2.17) is not crucial; however, if the energy dependence of the cross-section is known in more detail and, for example, resonances appear near the threshold energy then the integration of (2.15) has to be performed numerically (Meyer-Prüssner & Demmig 1979). Whereas most of the cross-section constants of the krypton reactions are known from previous studies (Meißner 1988; Krauß-Varban 1985; Fröbe 1981) none of the C–Kr cross-sections were known originally. Finally, the reverse rate coefficients are determined by the principle of detailed balancing.

3. Model computations

In order to reduce the number of reactions to the really relevant ones we carried out a sensitivity analysis. The following reaction rates gave only minor contributions: $R^{*}_{C^0C^0}$, $R^{+}_{C^*C^0}$, $R^{+}_{C^0C^0}$, $R^{*}_{K^0K^*}$, $R^{+}_{K^*K^*}$, $R^{*}_{K^0C^0}$, $R^{+}_{K^*C^0}$, $R^{+}_{K^0C^0}$, $R^{+}_{K^0e}$, $R^{+}_{C^0e}$ and $R^{+}_{C^0K^0}$, and thus

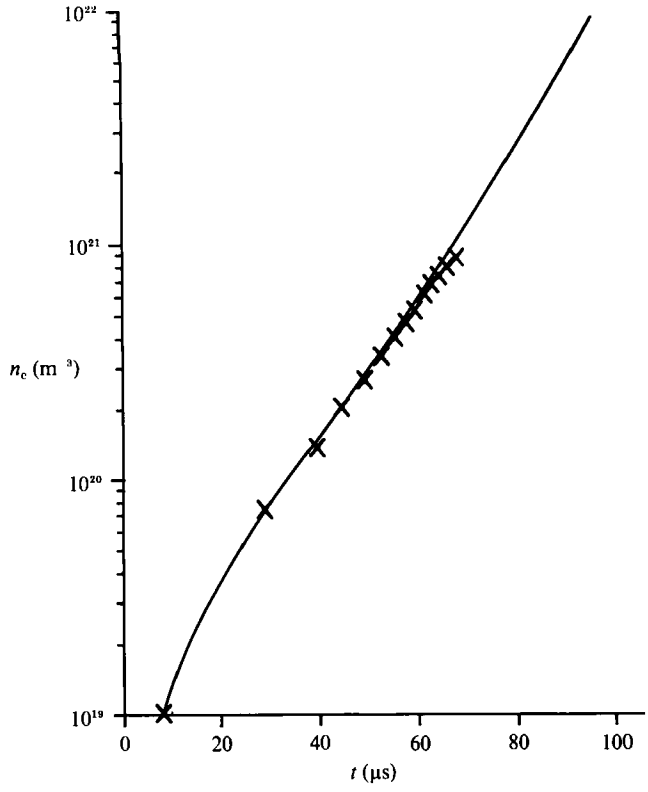

FIGURE 2. Comparison between measured (×) and computed (——) electron densities at a fixed measurement station for an impurity concentration of 37.5 p.p.m. and a temperature of 9626 K.

have been omitted in the rate equations. This result is mainly due to the small particle densities of C and Kr* in conjunction with relatively large threshold energies. In this context we emphasize that in many cases the contribution of $R^{+}_{C^{*}e}$ to the electron density is negligibly small (see (2.5)). But on the other hand this reaction rate plays an important role in the computation of the carbon particle densities ((2.2), (2.4) and §4).

We utilized a Lagrangian method for the numerical treatment of the gas dynamic equations (Hoskin 1964). The rate equations, being stiff, have been discretized according to a second-order process given by Steihaug and Wolfbrandt (Scraton 1981). For the incorporation of the rate equations into the non-equilibrium flow equations we refer to Demmig (1983*b*, 1978) and Meißner (1988). We chose the same step width for the integration of the gasdynamic and rate equations in order to attain a high degree of stability and accuracy. The results can be shown along a particle trajectory as well as at a fixed measurement station.

The choice of the initial value of the electron temperature only affects the development of the T_e values for a small number of computation steps (Hoffert & Lien 1967). In order to minimize this effect we compute the initial electron temperature by an extra computational step solving the electron energy equation. For this procedure we assume a very small initial particle concentration (e.g. 1.0×10^{-12}) of excited atoms, ions and electrons.

In order to find the unknown cross-section constants $C^{*}_{K^{0}K^{0}}$, $C^{*}_{C^{0}K^{0}}$, $C^{+}_{C^{*}K^{0}}$ and $C^{+}_{K^{0}K^{0}}$ we compared our model computations with experimental electron density profiles at

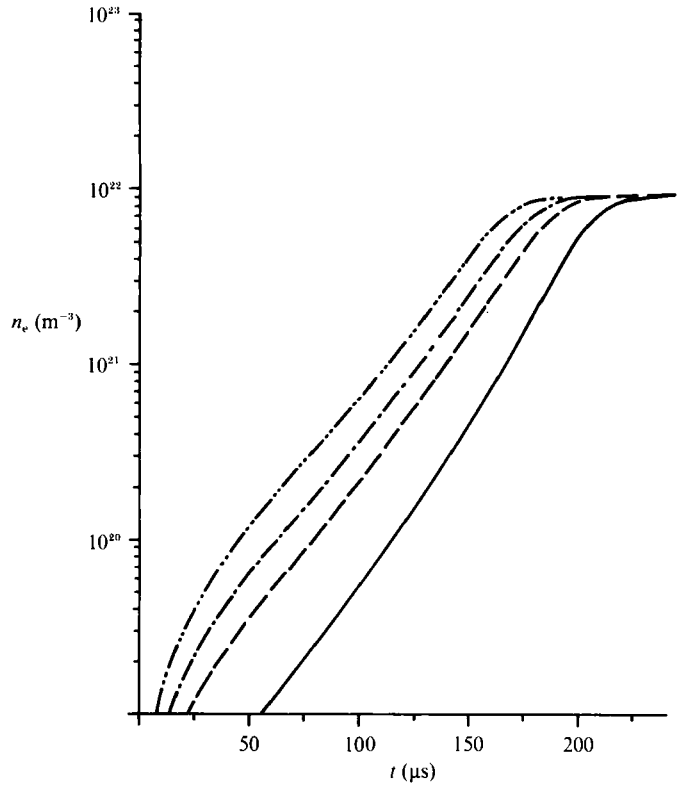

FIGURE 3. Dependence of the electron density on the impurity concentration at a fixed measurement station for a temperature of 8028 K: ——, 0 p.p.m; – – –, 20 p.p.m; –·–·, 40 p.p.m; —·· ··—, 80 p.p.m.

a specific measurement station measured by Fröbe, Müller & Bötticher (1983) using an HCN Mach Zehnder Laserinterferometer. Since atom–atom collisions dominate the electron production in the initial relaxation zone (figure 5) we adjusted our computations to measured electron densities at the start of the ionization relaxation. One result can be seen in figure 2. There is good agreement between measured and computed electron densities in the initial relaxation zone. In order to extend the experimental data base we used measured electron density profiles (Fröbe 1981; Ernst 1982; Schneider 1984) covering a relatively large range of plasma temperatures and impurity concentrations (§2). For our model computations we found the following set of cross-section constants, in m^2/J:

$$C^*_{K^0e} = 5.2\times10^{-3}, \quad C^*_{K^0K^0} = 3.0\times10^{-6},$$
$$C^+_{K^+e} = 4.0, \quad C^+_{K^+K^0} = 0.5,$$
$$C^*_{C^0e} = 0.1, \quad C^+_{K^0K^0} = 6.5\times10^{-6},$$
$$C^+_{C^+e} = 5.0, \quad C^*_{C^0K^0} = 6.7\times10^{-4},$$
$$C^+_{C^+K^0} = 1.5.$$

The constants $C^*_{K^0e}$, $C^+_{K^+e}$ and $C^+_{K^+K^0}$ are well known from many previous studies (Meißner 1988; Krauß-Varban 1985; Fröbe 1981). Furthermore, utilizing several theoretical works we were able to find values of $C^*_{C^0e}$ and $C^+_{C^+e}$ (Thomas & Nesbet 1976; Ganas 1981; Vriens & Smeets 1980).

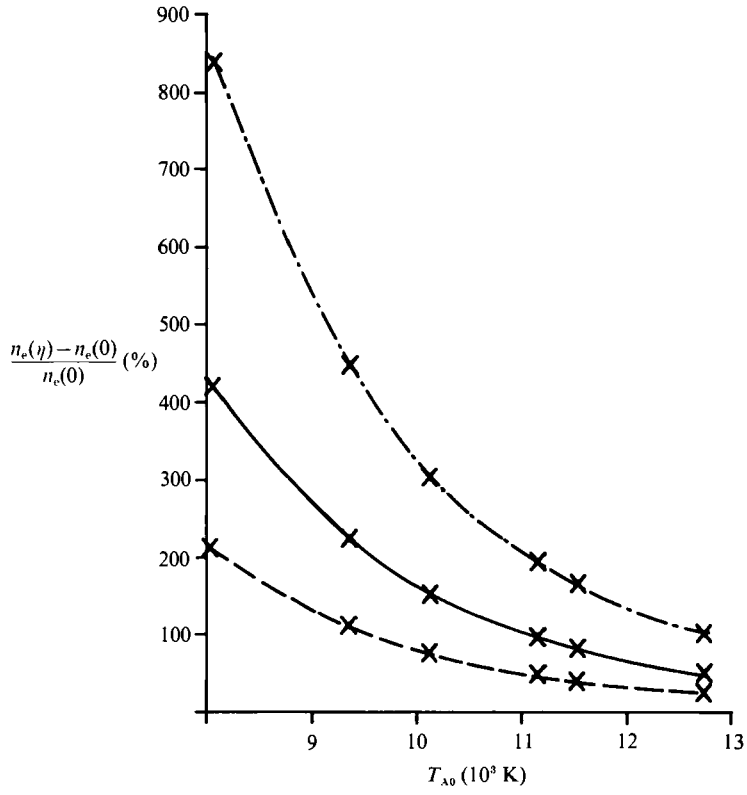

FIGURE 4. The relative electron density difference as a function of temperature for three different impurity concentrations at a fixed measurement station, 6 μs after the shock front has passed: ---, 10 p.p.m; ——, 20 p.p.m; —·—, 40 p.p.m; ×, computed data points.

While the mean momentum transfer cross-section of elastic electron–krypton collisions is known from the data of Devoto (1969), there are no literature data for electron–carbon collisions. Therefore we simply assume a constant value for this cross-section, which we were able to estimate by utilizing the corresponding data of elastic electron–oxygen collisions from Itikawa (1974). A variation of this cross-section value by two orders of magnitude shows only a negligible effect on the relaxation process. This weak sensitivity is due to the small concentration of carbon atoms and their relatively fast ionization by inelastic C–Kr collisions in the initial relaxation zone (figure 5).

4. Results

Figure 3 shows computed electron density profiles at a fixed measurement station for a temperature of 8028 K. A comparison between the 80 p.p.m. profile and the 0 p.p.m. profile shows a difference in the electron density of about one order of magnitude during the relaxation process. This enhancement of the electron production caused by the carbon atoms shortens the relaxation time by about 20%. In comparison Glass, Liu & Tang (1977) using a hydrogen impurity concentration of 0.38% found a 50% reduction of the relaxation time. These results demonstrate the strong influence of p.p.m. carbon impurities on the ionization relaxation in krypton shock waves. Figure 4 shows the relative difference of the electron density values $(n_e(\eta)-n_e(0))/n_e(0)$ of model computations at assumed impurity concentrations η

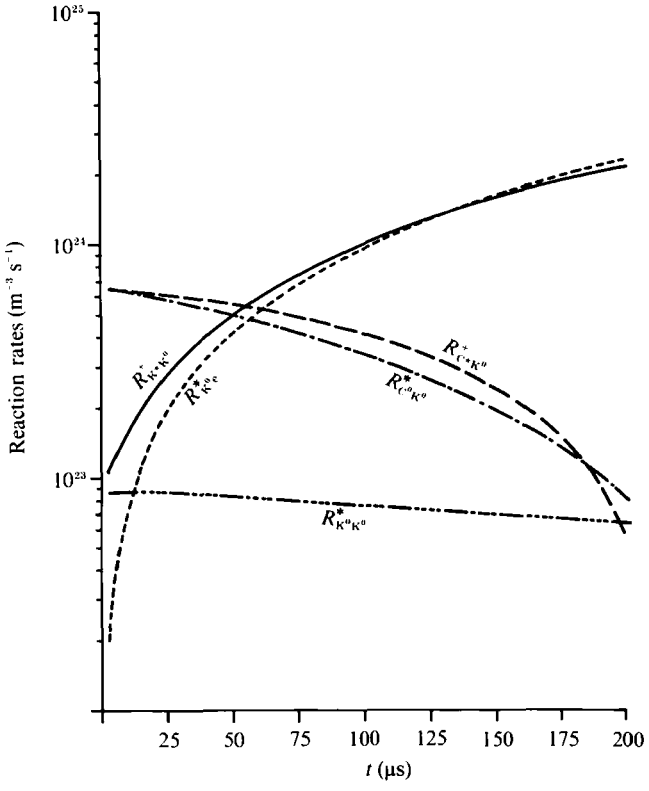

FIGURE 5. Reaction rates along a particle trajectory for an impurity concentration of 37.5 p.p.m. and a temperature of 8224 K.

and a model computation with $\eta = 0$ p.p.m. These values plotted versus the plasma temperature are taken 6 μs after the shock front has passed a specific measurement station. We chose this early moment in order to make use of the strong influence of the impurity atoms in the initial relaxation zone (figure 5). The enhancement effect is larger for lower temperatures. In these cases the threshold energies for krypton excitation and ionization, which are higher than those for carbon atoms, cause a slower developing krypton relaxation.

In order to study the impurity effect of carbon in more detail we computed several partial reaction rates along a particle trajectory. For a plasma temperature of 8224 K and an impurity concentration of 37.5 p.p.m. the result is shown in figure 5. As can be seen, in the initial relaxation zone the two partial rates $R^{*}_{C^{0}K^{0}}$ and $R^{+}_{C^{+}K^{0}}$ dominate the other ones including $R^{*}_{K^{0}K^{0}}$ and $R^{+}_{K^{+}K^{0}}$.

Figure 6 shows all relevant impurity-atom reaction rates including the variation of the carbon ion density $n_{C^{+}}$ and the density of ground-state carbon atoms $n_{C^{0}}$ along a particle trajectory for a temperature of 13248 K and a concentration of 16.2 p.p.m. In the initial relaxation zone there is a steep increase in the carbon ion density and at the same time a marked decrease in the ground-state carbon atoms. This very efficient excitation and ionization of carbon atoms is caused by the inelastic C–Kr collision rates $R^{*}_{C^{0}K^{0}}$ and $R^{+}_{C^{+}K^{0}}$ (figure 6). This effect in conjunction with an increasing electron density (figure 3) produces a negative value of the C–e rates $R^{+}_{C^{+}e}$ and $R^{*}_{C^{0}e}$. This means that the rate of the inverse process is higher than the corresponding forward rate. While $n_{C^{+}}$ reaches its maximum value, being higher than the local

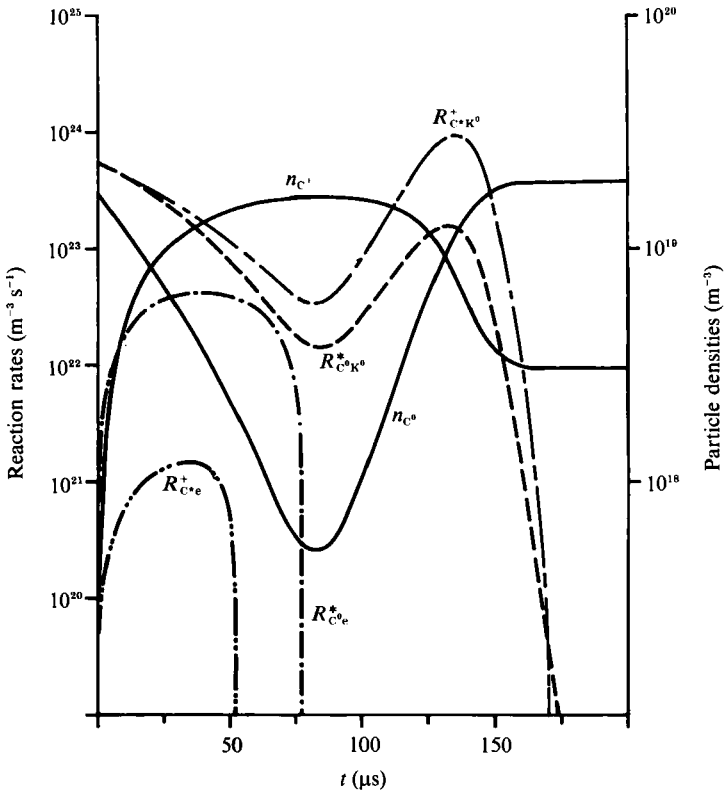

FIGURE 6. Carbon reaction rates and carbon particle densities along a particle trajectory for an impurity concentration of 16.2 p.p.m. and a temperature of 13248 K.

thermodynamic equilibrium (LTE) value, the ground-state carbon density is passing through a minimum. At this instant $R^{*}_{C^{0}e}$ is equal to $-R^{*}_{C^{0}K^{0}}$, and $R^{+}_{C^{+}e}$ to $-R^{+}_{C^{+}K^{0}}$, respectively ((2.2), (2.3)). From now on the electronic reaction rates are higher than the corresponding C–Kr rates. This effect causes a decrease of $n_{C^{+}}$ and simultaneously an increase of $n_{C^{0}}$ until LTE is reached ((2.2), (2.3)). The maximum of $n_{C^{+}}$ during the relaxation process is mainly due to the considerably lower excitation energy of carbon atoms in comparison to the krypton excitation energy.

We carried out a sensitivity analysis of the cross-section constants $C^{*}_{C^{0}e}$ and $C^{+}_{C^{+}e}$. A variation of about two orders of magnitude does not affect the qualitative development of $n_{C^{+}}$ and $n_{C^{0}}$. In this situation it would be desirable to have experimental data regarding, for example, the carbon ion density in order to verify the results predicted by our model computations. The higher LTE value of $n_{C^{0}}$ in comparison to its value at $t = 0$ is caused by the strong decrease in the heavy particle temperature in the final stage of the relaxation process (figure 7). As a result a marked increase in the total heavy particle density will occur.

Since the mass ratio of carbon and krypton particles is about one to seven the energy transfer between heavy particles and electrons is increased in comparison to the pure krypton gas. This stronger energy coupling causes a stronger increase of the electron temperature as can be seen in figure 7. In the initial relaxation zone the electron temperature for 80 p.p.m. is lower in comparison to the pure Krypton test gas owing to inelastic electron–carbon excitation collisions. A relatively high value of the corresponding cross-section constant and the lower excitation energy of carbon

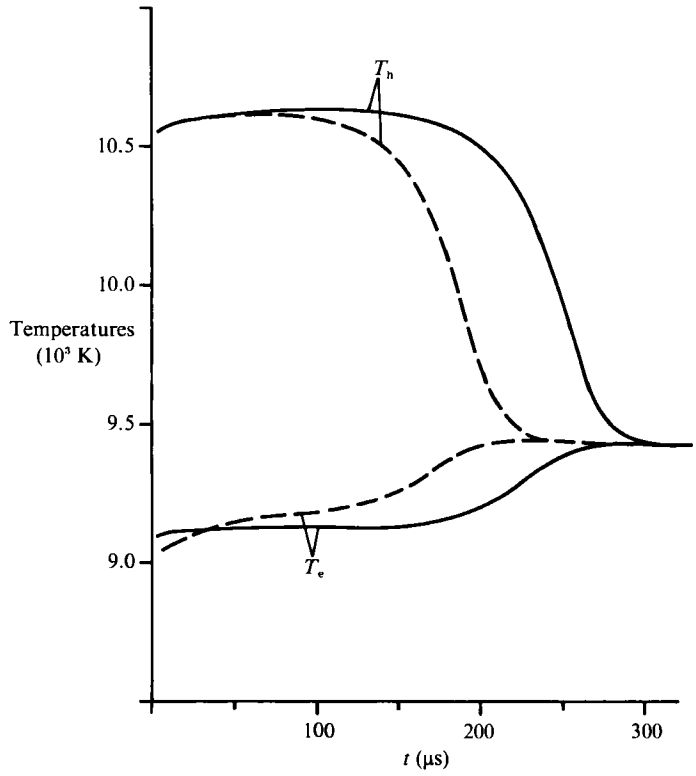

FIGURE 7. The influence of the impurity concentration on the heavy particle T_h and electron T_e temperatures along a particle trajectory: ——, 0 p.p.m; – – – –, 80 p.p.m.

atoms in comparison to krypton atoms are responsible for this effect. Despite the more efficient energy transfer between carbon particles and electrons in elastic collisions the main effect of carbon impurities on both temperatures is due to the additional electron production (figure 3) which causes an earlier onset of the electron avalanche effect. Consequently, the drastic decrease in the heavy particle temperature and the stronger, simultaneous increase in the electron temperature occurs earlier, too (figure 7).

Usually the effect of impurities on the relaxation is assumed to be small, and is roughly taken into account only in an indirect way. The Kr atom–atom excitation cross-section constant $C^*_{K^0K^0}$ is adjusted to the measured electron density of the initial relaxation zone in order to achieve a fairly good approximation of a pure krypton reaction model. Consequently, $C^*_{K^0K^0}$ depends on the impurity concentration η and the plasma temperature T_{A0} (figure 8).

In contrast, our model allows for the relevant impurity atom reactions and yields a value of the true Kr–Kr excitation cross-section constant. By comparing computational results of the Kr–C model for different degrees of impurities and different temperatures with those for the simplistic pure Kr model we were able to explain the above-mentioned dependence of the Kr–Kr excitation cross-section constant on the impurity concentration and the plasma temperature. For three different temperatures the result is illustrated in figure 8. For clarity each curve connects the values obtained for $C^*_{K^0K^0}$. The cross-section constant increases nearly proportional to the impurity concentration. The higher values for lower temperatures

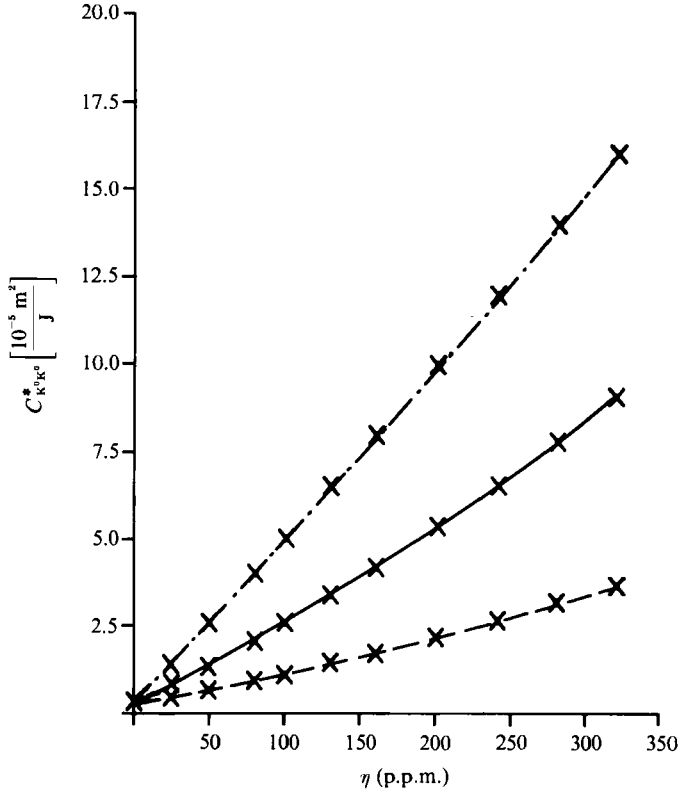

FIGURE 8. The Kr–Kr excitation cross-section constant as a function of impurity concentration for three different temperatures: – – –, 12740 K; ——, 10117 K; —·—·, 8028 K; ×, computed data points.

are just reflecting the temperature-dependent influence of carbon impurities on the ionization relaxation in rare-gas shock waves.

5. Discussion

Most investigations concerned with the role of impurities in ionization relaxation processes suffer from the drawback of neglecting the influence of wall boundary layers which causes an additional increase in the electron production and thus an additional decrease in the relaxation time. We would like, however, to mention two of the investigations because of their significance in the impurity discussion. Igra (1972) gives a thorough qualitative discussion of the influence of impurities on non-equilibrium shock tube flows. Though Jones & McChesney (1966) neglected three-body recombination processes, necessary for a complete relaxation model, their work is an attempt to integrate impurity reactions into the theoretical description of ionization relaxation. Also, in order to describe the ionization process of argon atoms and impurities these authors assume a quasi one-step mechanism which is strictly applicable only to a special group of impurities like rare-gas atoms or hydrogen.

The main interest of our work is the explanation of the above-mentioned decrease of the krypton–krypton excitation cross-section constant as the experimental technique was improved. Consequently, we developed a two-step model for both krypton test gas atoms and carbon impurity atoms. Our results not only confirm the

more or less qualitative findings of the above-mentioned works but also give detailed information about the variation of physical quantities such as, for example, the electron density throughout the relaxation zone. The enhancement effect of the electron production in the initial relaxation zone due to impurities in the low p.p.m. range is quite similar in structure to the very strong catalysing effect of minute hydrogen concentrations in the H_2+D_2 exchange reaction, reported by Lifshitz & Bidani (1981).

For a comparison between model computations and experimental results one can utilize the effect of impurities on, for example, the relaxation length or the development of the electron density during the ionization relaxation process. From figure 3 it follows that the electron density reacts much more sensitively to carbon impurities than the relaxation length, the latter being nearly proportional to the relaxation time in the case of a weak unsteady shock wave. Since in our work we are mainly interested in the effects of carbon impurities in the low p.p.m. range on the reaction kinetics it is necessary to adjust our computations to measured electron densities and not to experimentally determined relaxation lengths.

On the basis of a pure krypton model Fröbe, Müller & Bötticher (1983) obtained a value of the krypton–krypton excitation cross-section constant from measured electron densities. The variation of their value between 1.3×10^{-5} and 2.2×10^{-5} m^2/J is due to the different temperatures (7500 K $< T_{A0} <$ 9900 K) of the experiments. Since the authors report a carbon impurity concentration of 37 p.p.m. there is very good agreement between their values and those obtained from our krypton–carbon model (figure 8).

One has to keep in mind, however, that the determination of cross-sections by shock tube experiments is subject to systematical errors, as has been discussed in more detail by, for example, Demmig (1983*a*). In addition to the boundary-layer influence, there is also the possible deviation of the electron velocity distribution from the Maxwellian. Meyer-Prüssner & Demmig (1979) found that, especially in the initial relaxation zone, the high-energy tail crucial for the excitation/ionization might not be replenished fast enough. A first attempt to take this effect into account by using the analytic Shaw–Mitchner–Krueger (SMK) distribution (Shaw, Mitchner & Krueger 1970) was not successful because the mixture Kr+C does not fulfil the requirements of SMK. The generalization of Meyer-Prüssner's method to mixtures to compute the electron velocity distribution function numerically, as in Meyer-Prüssner & Demmig (1979), seems feasible. This work is under way.

Furthermore it is desirable to have more information about the two decisive impurity reactions $R^{*}_{C^0K^0}$ and $R^{+}_{C^*K^0}$ in order to check the corresponding cross-section constants coming out of our work.

We thank W. Bötticher and the members of the experimental shock tube group of our institute for providing measured electron density values and K. Haupt for drawing the figures.

REFERENCES

Demmig, F. 1978 The computation of one-dimensional unsteady non-equilibrium flows with a method of characteristics utilizing exponential fitting. *Comput. Phys. Commun.* **14**, 7.

Demmig, F. 1983*a* Models for non-equilibrium flows in real shock tubes. *Proc. 14th Intl Symp. on Shock Tubes and Waves, Sydney* (ed. R. D. Archer & B. E. Milton), p. 51.

Demmig, F. 1983*b* Investigation of ionization relaxation in shock tubes; merits and limitations. *Proc. 14th Intl Symp. on Shock Tubes and Waves, Sydney*, p. 744.

DEVOTO, R. S. 1969 Transport coefficients of partially ionized Krypton and Xenon. *AIAA J.* **7**, 199.

ERNST, G. 1982 Absorption spectroscopic investigations for the reaction kinetics of excited Krypton atoms in shock waves using a single-mode dye laser (in German). Doctorial thesis, University of Hannover.

FRÖBE, U. 1981 Investigation of ionization relaxation in shock heated Krypton using an HCN-Laser-Interferometer (in German). Doctorial thesis, University of Hannover.

FRÖBE, U., MÜLLER, B.-H. & BÖTTICHER, W. 1983 Ionization relaxation in shock-heated Krypton at electron densities from $1\text{–}50 \times 10^{19}$ m^{-3}. *J. Phys.* B: *Atom. Molec. Phys.* **16**, 4259.

GANAS, P. S. 1981 Electron impact excitation cross sections for Carbon. *Physica* C**104**, 411.

GLASS, I. I., LIU, W. S. & TANG, F. C. 1977 Effects of Hydrogen impurities on shock structure and stability in ionizing monoatomic gases: 2. Krypton. *Can. J. Phys.* **55**, 1269.

HOFFERT, M. I. & LIEN, H. 1967 Quasi-one-dimensional, nonequilibrium gas dynamics of partially ionized two-temperature Argon. *Phys. Fluids* **10**, 1769.

HOSKIN, N. E. 1964 Solution by characteristics of the equations of one-dimensional unsteady flow. *Meth. Comput. Phys.*: *Adv. Res. Applics* **3**, 265.

IGRA, O. 1972 Impurities effects on the ionization zone behind strong normal shock waves in monoatomic gas. *Israel J. Technol.* **10**, 153.

ITIKAWA, Y. 1974 Momentum-transfer cross sections for electron collisions with atoms and molecules. *Atom. Data Nucl. Data Tables* **14**, 1.

JONES, N. R. & MCCHESNEY, M. 1966 Ionization relaxation in slightly impure Argon. *Nature* **209**, 1080.

KRAUß-VARBAN, D. 1985 Radiation transport in rare gas shock waves and the model description of excitation and ionization in the precursor (in German). Doctorial thesis, University of Hannover.

KRAUß-VARBAN, D. & DEMMIG, F. 1984 Model calculations of the ionization relaxation and radiative cooling in unsteady Krypton and Xenon shock waves. *J. Fluid Mech.* **149**, 375.

LIFSHITZ, A. & BIDANI, M. 1981 The effect of minute quantities of impurities on shock tube kinetics. *Proc. 13th Intl Symp. on Shock Tubes and Waves, Niagara Falls* (ed. C. E. Treanor & J. G. Hall), p. 602.

MEIßNER, J. 1988 The computation of a two dimensional non-equilibrium flow afflicted with friction behind an unsteady plane shock wave (in German). Doctorial thesis, University of Hannover.

MEYER-PRÜSSNER, R. & DEMMIG, F. 1979 Ionization relaxation in shock tubes taking into account a non-maxwellian electron velocity distribution. *Proc. 12th Intl Symp. on Shock Tubes and Waves, Jerusalem* (ed. A. Lifshitz & J. Rom), p. 197.

SCHNEIDER, J. M. 1984 Particle density and collision frequency of electrons during the ionization relaxation in shock heated Krypton–Helium mixtures. A comparison of model computations and measurements using HCN- and CO_2-lasers (in German). Doctorial thesis, University of Hannover.

SCRATON, R. E. 1981 Some L-stable methods for stiff differential equations. *Intl J. Comput. Maths* B**9**, 81.

SHAW, J. F., MITCHNER, M. & KRUEGER, C. H. 1970 Effects of nonelastic collisions in partially ionized gases; I. Analytical solutions and results. *Phys. Fluids* **13**, 325.

THOMAS, L. D. & NESBET, R. K. 1976 Low-energy electron scattering by atomic Carbon. *Phys. Rev.* A **12**, 2378.

VRIENS, L. & SMEETS, A. H. M. 1980 Cross-section and rate formulas for electron-impact ionization, excitation, deexcitation, and total depopulation of excited atoms. *Phys. Rev.* A**22**, 940.